Medicinal & Aromatic Plants
ISSN: 2167-0412

Rejeeth et al., Med Aromat Plants 2014, 3:3
DOI: 10.4172/2167-0412.1000163

Research Article Open Access

Biosynthesis of Silver Nanoscale Particles Using *Spirulina platensis* Induce Growth-Inhibitory Effect on Human Breast Cancer Cell Line MCF-7

Chandrababu Rejeeth[1]*, Bojan Nataraj[2], Raju Vivek[1] and Marimuthu Sakthivel[2]

[1]*Proteomics and Molecular Cell Physiology Lab, Department of Zoology, School of Life Sciences, Bharathiar University, Coimbatore, Tamil Nadu - 641 046, India*
[2]*Department of Zoology, School of Life Sciences, Bharathiar University, Coimbatore, Tamil Nadu - 641 046, India*

Abstract

A biological method was used to synthesize stable silver nanoparticles that were tested against MCF-7 cells are reported. The structure and percentage of synthesized nanoparticles was characterized by using ultraviolet spectrophotometry, X-Ray diffraction, Fourier transform infrared spectroscopy, and scanning electron microscopy methods. The zeta potential value of -36 mV revealed the stability of biosynthesized AgNPs. The *in vitro* screening of the AgNPs showed potential cytotoxic activity against human breast cancer cell and normal breast epithelial cells the inhibitory concentration (IC_{50}) were found to be 20, 40, 60 and 80 µg/ml for AgNPs against MCF-7 and HBL-100 cells at 24 and 48 h incubation respectively. An induction of apoptosis was evidenced fluorescence microscopy. These results suggest that AgNPs may exert its anti proliferative effects on breast cancer cell line by suppressing its growth, arresting the G0/G1-phase, reducing DNA synthesis.

Keywords: Algal extract; AgNPs; MCF-7; Apoptosis; Breast cancer

Introduction

Nanotechnology, involves design, synthesis, and manipulation of structures in particles with dimension can be in the range from 10 nm to 1000 nm. Physical and chemical entities of plant and microbial origins have the ability to generate nanoscale value properties. Currently, nanobiotechnology represents an economic alternative for chemical and physical methods for the synthesis of nanoparticles [1]. Development of technologies for producing nanoparticles, because of their key role in the future world could be one of the most valuable findings of human being. Nanoparticles have a wide range of use in different fields of industry, medicine and basic science. Utilizing nanoparticles especially silver nanoparticles in production of cosmetics, detergents and hygienic goods is widely practiced. The Silver nanoparticles (AgNPs) are reported to be nontoxic to human and most effective against bacteria, viruses, and other eukaryotic microorganisms at very low concentration and without any side effects [2].

High demands for nanoparticles have been led to the production of them in large scales. So a wide range of industrial methods have been developed to synthesize metal nanoparticles. Some of these procedures are involved using toxic solvents or high energy consumption. This leads to a growing awareness of the need for developing clean, nontoxic and environmentally friendly procedures. An attractive possibility is employing microorganisms, like bacteria [3], fungi [4], and alga [5] in nanomaterial production. Several methods were employed for the synthesis of AgNPs ranging from chemical procedures [6], radiation [7], electrochemical [8] and photochemical methods [9]. Recently, biological synthesis of nanoparticles is in application for its eco-friendly mode of synthesis with passable biomedical applications [10,11]. In a recent study, the cytotoxic activity of Melia azedarach was reported against human lung adenocarcinoma cell lines [12]. In most cases, the evaluation of the anti-cancer potential of crude extracts from different sea organisms has been carried out by in vitro cytotoxicity tests in malignant cell cultures [13]. Hundreds of potential anti-tumor agents have been isolated from marine origin especially from marine algae [14]. *In vitro* study is an important means to evaluate the mechanisms of toxicity caused by nanomaterials. Different cell types have been investigated for cytotoxicity of AgNPs, including NIH 3T3 fibroblast cells [15], HeLa cells [16] and human glioblastoma cells [17]. The mechanisms for AgNPs induced toxicity may be related with mitochondrial damage, oxidative stress, DNA damage and induction of apoptosis [18]. The present study involves with the synthesis and characterization of AgNPs using a *Spirulina platensis* which were further characterized using UV–vis spectroscopy, XRD, FTIR, SEM, DLS, Zeta potential and its effect on cell viability was also studied to reflect the cytotoxicity evaluating the AgNPs against human breast cancer cells (MCF-7) and normal breast epithelial cells (HBL-100) *in vitro*.

Materials and Methods

Collection of alga and Preparation of pure algal extract

The *Spirulina platensis* pure culture was obtained from Antenna Green Trust, Kadachanenthal, Madurai, Tamilnadu India. The pure algal extract (PAE) was prepared by adding 1g of algal powder into 100 ml of distilled water and boiled for 5 min. The boiled extract was filtered through Whatman No.1 Filter paper and the supernatant was used and stored at 4°C for further process.

Synthesis of silver nanoparticles

Biological synthesis of AgNPs was carried out by typically synthesis process. Briefly, In the of silver nanoparticles, add 10 ml of pure algal extract into the 90 ml of 1 mM of silver nitrate solution in 250 ml conical flask and kept in different temperature such as 30°C, 40°C, 60°C, 70°C, 80°C, 90°C and 100°C under mechanically stirring. The colour change was noted and nanoparticles formation was monitored using UV-vis Spectrophotometer periodically.

***Corresponding author:** Chandrababu Rejeeth, Proteomics and Molecular Cell Physiology Lab, Department of Zoology, School of Life Sciences, Bharathiar University, Coimbatore, Tamil Nadu - 641 046, India, Tel: +91 9486138085; E-mail: crejee@gmail.com

Received June 13, 2014; **Accepted** July 22, 2014; **Published** July 26, 2014

Citation: Rejeeth C, Nataraj B, Vivek R, Sakthivel M (2014) Biosynthesis of Silver Nanoscale Particles Using *Spirulina platensis* Induce Growth-Inhibitory Effect on Human Breast Cancer Cell Line MCF-7. Med Aromat Plants 3: 163. doi: 10.4172/2167-0412.1000163

Characterization of silver nanoparticles

The optical properties of AgNPs were monitored as a function of time in 10 mm optical path-length-quartz-cuvettes with a Shimadzu, UV–Vis range 3600 spectrophotometer. Samples were diluted 5 times with distilled water before being measured. The morphology of the particles was examined by scanning electron microscope (FEI QUANTA-200 SEM). DLS measurements were performed at room temperature (25 ± 2°C), with a Zetasizer Nano ZS (Malvern Instruments) equipped with a He–Ne laser (λ=633 nm) and a backscatter detector at a fixed-angle of 173°. Zeta potential measurements were carried out using a Malvern Instrument Zeta Sizer Nano not only to compare the surface charge of the nanoparticles but also to evaluate their hydrophilicity. Zeta potential is measured by the capillary electrophoresis method. The surface groups of the nanoparticles were qualitatively confirmed by using Fourier transform infrared (FTIR) spectroscopy (Stuart 2002), with spectra recorded by a Perkin-Elmer Spectrum 2000 FTIR spectrophotometer. X-ray diffraction (XRD) using Cuka radiation (PANanlytical X'pert Pro MPD diffractometer) allowed us to determine the crystalline structure of the silver nanoparticles. Powder X-ray analysis was made by using a Philips PW 1050/37 diffractometer, operating at 40 kV and 30 mA, with a step size of 0.02° (2θ) [19].

Cell culture

The breast cancer cells (MCF-7) and normal breast epithelial cells (HBL-100) were maintained in Dulbecco's modified eagles medium (DMEM) supplemented with 2 mM L-glutamine and balanced salt solution adjusted to contain 1.5 g/L Na_2CO_3, 0.1 mM nonessential amino acids, 1mM sodiumpyruvate, 2 mM L-glutamine, 1.5 g/L glucose, 10 mM (4-(2-hydroxyethyl)-1-piperazineethane sulfonic acid), and 10% fetal bovine serum (GIBCO, USA). Penicillin and streptomycin (100 IU/100 µg) were adjusted to 1 mL/L. The cells were maintained at 37°C with 5% CO_2 in a humidified CO_2 incubator [20].

In vitro cytotoxicity of synthesized AgNPs

Cells were cultured and ~1×10^4 cells/wells were seeded into 96 well tissue culture plates and incubated for 48 h. Both MCF-7 and HBL-100 cells were treated with series of 10-100 µg/mL concentrations of green synthesized AgNPs. The treated cells were incubated for 24 h and 48 h for cytotoxicity analysis. The cells were then subjected for MTT assay. The stock concentration (5 mg/mL) of MTT-(3-(4,5-dimethylthiazol-2-yl)-2,5-diphenyltetrazolium bromide, a yellow tetrazole) was prepared and 100 µL of MTT was added in each AgNPs treated wells and incubated for 4 h. Purple color formazone crystals were observed and these crystals were dissolved with 100 µL of dimethyl sulphoxide (DMSO), and read at 620 nm in a multi well ELISA plate reader (Thermo, Multiskan). OD value was subjected to sort out percentage of viability by using the following formula

$$\text{Percentage of viability} = \frac{\text{Mean OD value of experimental sample (AgNPs)}}{\text{Mean OD value of experimental control (untreated)}} \times 100$$

Morphological observation

Cells were grown (1×10^5 cells/cover slip) and incubated with AgNPs at their IC_{50} concentration and then they were fixed in methanol: acetic acid (3:1, v/v). The cover slips were gently mounted on glass slides for the morphometric analysis. Morphological changes of MCF-7 cells were analyzed under the Nikon (Japan) bright field inverted light microscopy at 40× magnification.

JC-1 staining

Approximately 5 µL of JC-1 dye mixture was mixed with 9 mL of cell suspension (1×10^5 cells/mL) on a clean microscopic cover slip. After incubation for 2–3 min, cells were visualized under fluorescence microscope (Nikon Eclipse, Inc., Japan) at 40× magnification with excitation filter at 488-510 nm. Percentage of apoptotic cells was determined by the following formula

$$\%\ \text{of apoptotic cells} = \frac{\text{Total number of normal and apoptotic cells}}{\text{Total number of apoptotic cells}} \times 100$$

DAPI (4,6-diamidino-2-phenylindole, dihydrochloride) staining

MCF-7 cells were treated with the above methods for 48 h, and then fixed with methanol: acetic acid (3:1, v/v) prior to washing with PBS. The washed cells were then stained with 1 mg/mL DAPI (4,6-diamidino-2-phenylindole, dihydrochloride) for 20 min in the dark. Stained images were recorded with fluorescent microscope with appropriate excitation filter.

Cell cycle analysis

Cell cycle distribution and percentage of apoptotic cells were performed by flow cytometry [21]. After treatment, floating cells in the medium were combined with attached cells collected by trypsinization. Cells were washed with cold PBS and fixed using 80% ethanol in PBS at -20°C. Fixed cells were pelleted and stained with propidium iodide (50 µg/ml) in the presence of RNase A (20 µg/ml) for 30 min at 37°C. About 10^4 cells were analyzed in a Becton Dickinson FAC scan flow cytometer. Cell cycle histograms were analyzed using cell Quest Software.

Statistical analysis

All measurements were made in triplicate and all values were expressed as the mean ± standard error of the mean. The results were subjected to an analysis by Student's t-test. The results were considered statistically significant if the p value was ≤0.05.

Results and Discussion

Synthesis of silver nanoparticles

Spirulina platensis were used for the reduction of $AgNO_3$ into nanoscale values, initially it was confirmed based on the colour change from colourless to yellowish brown and ruby red colour in solutions [22]. Temperature dependent reduction was observed by change in the colour of reaction mixture with an excitation of surface Plasmon resonance (SPR) observed at 420 nm in UV–visible spectrophotometer (Figure 1A). In our observations, the increase in reaction time increases the reduction process of AgNPs as noticed in the SPR peak at every 30 min interval (Figure 1B). The stability of the synthesized AgNPs was determined at room temperature for 30 days by UV spectrophotometer. Synthesized AgNPs shows good stability at room temperature (27 ± 3°C) without aggregation with an intense SPR peak at 420 nm after 30 days. The absorption peak varied as a function of reaction time and silver nitrate concentration. As the size of the particles decreased, the energy gap increased, and the absorption peak shifted to a higher energy level. The silver surface Plasmon resonance (SPR) band occurred at 424 nm and steadily increased in intensity as a function of time of reaction without any shift in the peak wavelength [22]. The surface plasmon peak we observed after the addition of A. squamosa extract, evidenced from the appearance of brownish yellow color and the λ_{max} appeared at 444 nm [23].

Characterization of silver nanoparticles

In SEM analysis, the synthesized green AgNPs shows less aggregation with particles are spherical in shape and the size ranges from 10 to 200

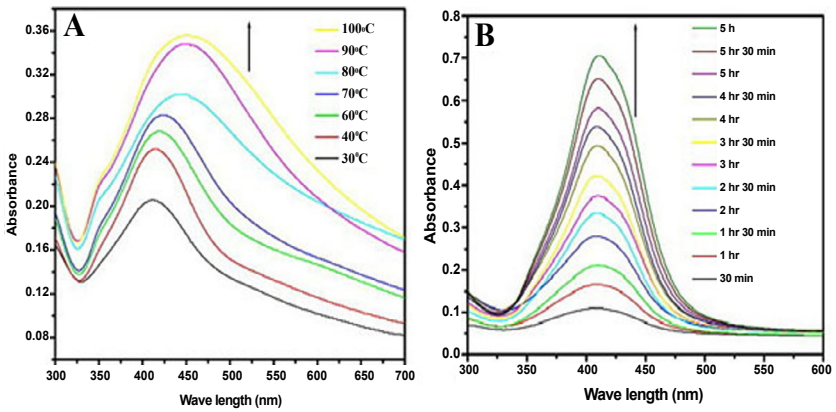

Figure 1: Effect of temperature and incubation time. (A) Effect of temperature on green AgNPs synthesis colour change in the reaction mixture and UV–visible spectra. (B) Effect of incubation time on green AgNPs synthesis at 90°C. Colour change in the reaction mixture and UV–visible spectra.

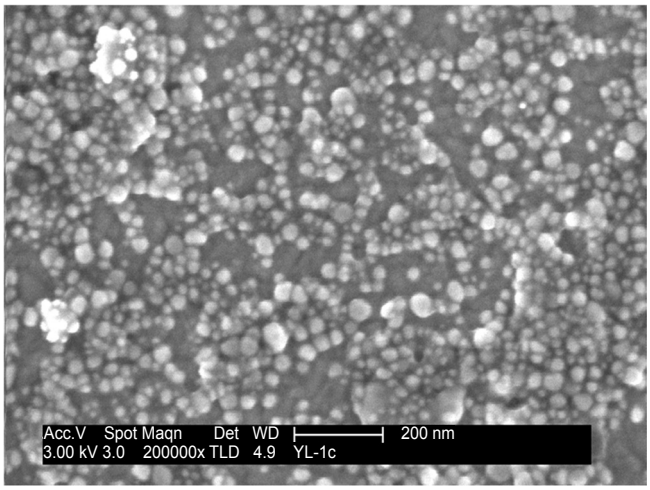

Figure 2: Topographical results of green AgNPs confirmed the range of particle size below 100 nm from SEM analysis.

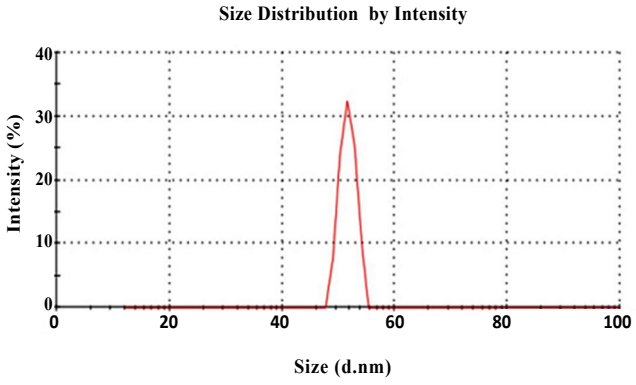

Figure 3: Size distribution analysis by DLS. The particle size distribution revealed that the particles range from 10–100 nm. The average particle size was found to be 50 nm.

nm in diameter (Figure 2). The green AgNPs size measured from the dynamic light scattering (DLS) intensity obeys Raleigh scattering and is proportional to the radius of the particle raised to the sixth power, then a small number of large particles can contribute in the increase

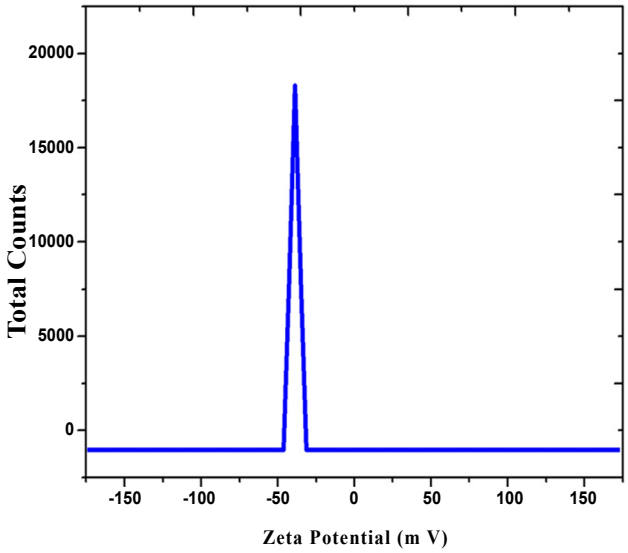

Figure 4: Zeta potential measurement of green synthesized AgNPs potential value of 48 mV.

of DLS size, resulting in recording an average size of 50 nm (Figure 3). Zeta potential measurements were also investigated for the systems and are shown in Figure 4. Zeta-potential varies by dissociation of surface groups in a wide range of electrolyte conditions. The zeta potential value for green AgNPs was -36 mV, The XRD patterns of synthesized AgNPs are shown in Figure 5. There were intense silver nanoparticle (AgNP) diffraction peaks at 38.10°, 44.44°, 64.47° and 77.53° 2θ, corresponding to facets 111, 200, 220 and 311 of the face-centered cubic crystal structure. Sathyavathi et al. (2010) reported diffraction peaks at 44.50°, 52.20°, and 76.7° 2θ, which correspond to the (111), (200), and (220) facets of the face-centered cubic crystal structure. Furthermore the result shows that the phytochemical constituents, particularly tannins protect the AgNPs from aggregation and thereby retain the long term stability of nanoparticles [24-26].

The FT-IR spectrum of the green AgNPs from *Spirulina platensis* showed strong absorption peaks at 3406, 2925, 1636, 1551, 1383, 1259, 1032 and 873 cm^{-1} which represents the various functional group like O-H stretching of alcohols and phenols, N-H group (amino acids), C-O

of carboxylic anions, O-H compounds (carboxylic acid), saturated C-O group and N-O stretching respectively (Figure 6) The absorption peak at 3460 cm^{-1} indicates the presence of N-H group (amino acids). The disappearance of secondary metabolites after the bioreduction of silver nanoparticles was also confirmed by FTIR spectroscopy and is thought to result from the reduction of Ag ions by the polyols, which themselves are oxidized to unsaturated carbonyl groups with a broad peak at 1650 cm^{-1} [27].

In vitro assessment of green AgNPs cytotoxicity

Silver nanoparticles as an antimicrobial agent, is gaining greater demand in medical applications. At the same time, there are only limited studies in the cytotoxic effects of green synthesized AgNPs, against cancer cell lines. MTT assay was used to assess the effect of AgNPs on proliferation of MCF-7 cells and HBL-100 cells. This is the first study to report the cytotoxicity of AgNPs synthesized using *Spirulina platensis* against breast cancer cell lines (MCF-7). In the present study, we investigated that the induction of apoptosis could be the possible mechanism for anti-proliferative activity of green synthesized AgNPs. The dose dependent cytotoxicity was observed in AgNPs treated MCF-7 cells. 50% of cell death, which determines the inhibitory concentration (IC_{50}) value of green synthesized AgNPs against MCF-7 cells holds at 60 µg/mL in 24 h and 30 µg/mL in 48 h (Figure 7a). Similar report of cytotoxicity was discussed by Sukirtha et al. [18] and Vivek et al. [23]. However the cytotoxicity effect of green synthesized AgNPs against HBL-100 did not exhibit significant cytotoxicity at lower concentration and cytotoxicity increases with increasing concentration by 80 µg/mL in 24 h and 60 µg/mL in 48 h (Figure 7b). A large number of *in vitro* studies indicated that the AgNPs are toxic to the mammalian cells. To be sure, our results also provide conclusive evidence for cytotoxic effect of green synthesized AgNPs against breast cancer MCF-7 cell line compared with HBL-100 normal breast cell line.

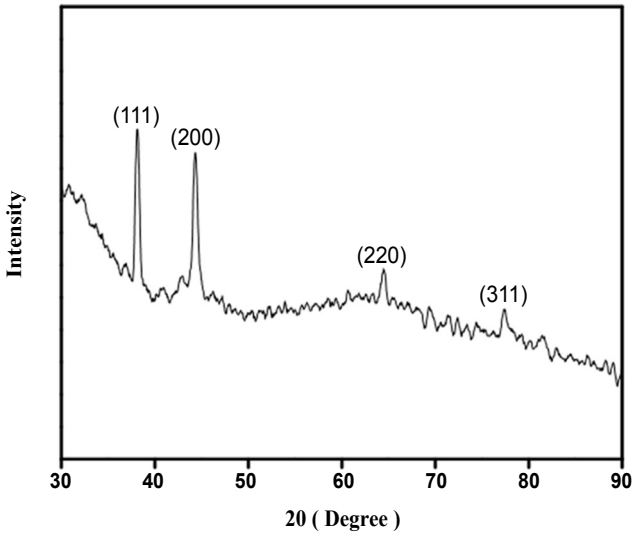

Figure 5: XRD pattern of green synthesized AgNPs exhibiting the facets of crystalline nature.

Induction of apoptosis by green synthesized AgNPs

Morphological analysis: The morphological changes were observed in AgNPs treated cells MCF-7 cells when compared with the untreated cells. The most recognizable morphological changes of AgNPs treated cells observed in this study was the cytoplasmic condensation, cell shrinkage, production of numerous cell surface protuberances at the plasma membrane and aggregation of the nuclear chromatin into dense masses beneath the nuclear membrane (Figure 8B and C).

Fluorescence microscopy: The induction of apoptosis, after the treatment with IC_{50} concentration of AgNPs was assessed by fluorescence microscopy the MCF-7 cell viability was observed by staining live and dead cells with DAPI and JC-1, respectively. Fluorescence stained breast cancer cells after treatment with the control (nontreated) Figure 8D and G respectively. Remarkable morphological changes were observed under the fluorescence microscope when cells were treated

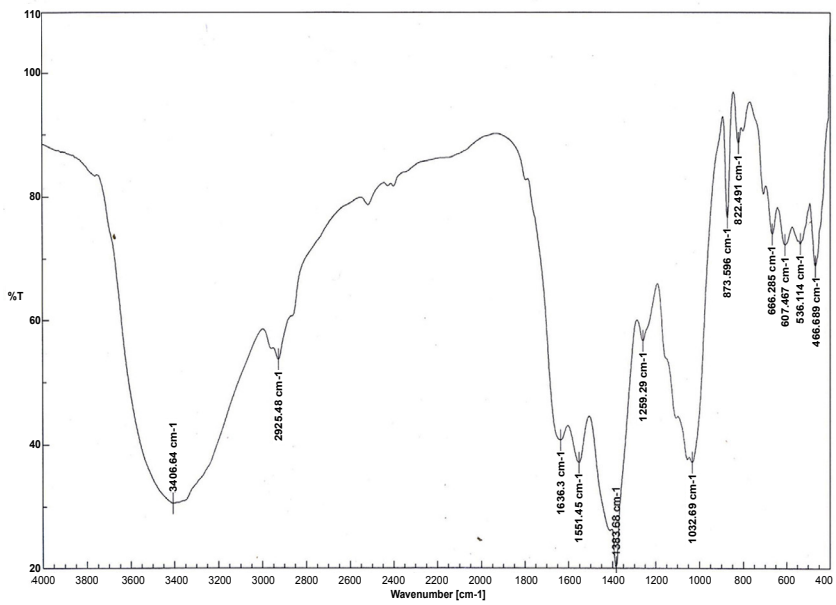

Figure 6: FT-IR spectra of green synthesized silver nanoparticles from *Spirulina platensis*.

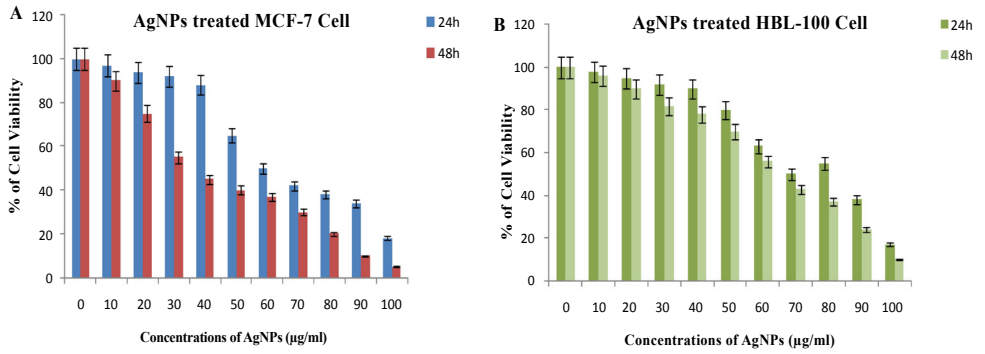

Figure 7: MTT assay results confirming the *in vitro* cytotoxicity effect of AgNPs against the MCF-7 and the normal HBL-100 cells for 24 h and 48 h respectively. (A) Cytotoxic effect of AgNPs on cancer cell line (MCF-7) and (B) Cytotoxic effect of AgNPs on normal cell line (HBL-100). The detected IC_{50} concentrations were 60 µg/ml and 30 µg/ml for MCF-7 and 80 µg/ml and 60 µg/ml for HBL-100 cells for 24 h and 48 h respectively. Data is expressed as mean ± SD of three experiments. Percentage of cytotoxicity is expressed relative to untreated controls (*significant $p < 0.05$).

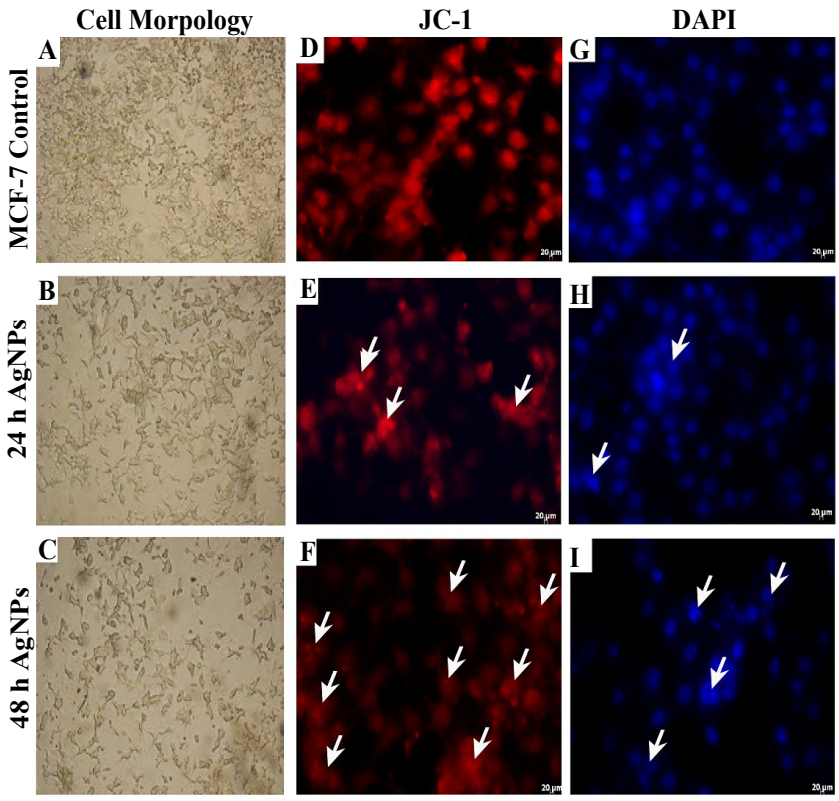

Figure 8: Bright field and fluorescence microscopy image of IC_{50} concentration of AgNPs treated on MCF-7 cells. Control cells of MCF-7 and cytotoxicity observed from bright field microscope (A, B and C). Fluorescence microscopy study of JC-1 and DAPI stained respective control cells.

with AgNPs Figure 8 E, F, H and I. In Figure 8D the number of cells remaining after treatment with the particles is less than the others. The MTT results also have shown that the greatest reduction in metabolic activity was produced by the treated cells, which is in agreement with the fluorescence microscopy images. Results showed that after 24 h and 48 h of incubation, AgNPs have the strongest adverse effect on viability compared to the control. In the fluorescence images, most of the cells appeared dead after treatment with AgNPs (Figure 8F and I). In contrast, treatment with control (nontreated) led to slate significant adverse effects in the cells; most of the cells are alive as shown in Figure 8A, D and G. This study indicates that nanoparticle-mediated morphological alteration may occur in the cells and to study these morphological changes at a higher level of resolution.

Effect of green AgNPs on cell cycle control of MCF-7: To investigate whether the green AgNPs affect regulation of cell cycle, flow cytometry was performed. Figure 9 shows that incubation of green AgNPs with MCF-7 cells for 48 h significantly reduced the DNA content, make them appear in the sub-G0/G1 region indicative of apoptosis, with consequent loss of cells in the G1 phase. 60.2% of cells were in sub G0/G1 phase, with 10.8% cells in the same phase in the respective control. Previous reports showed that analysis of the cell

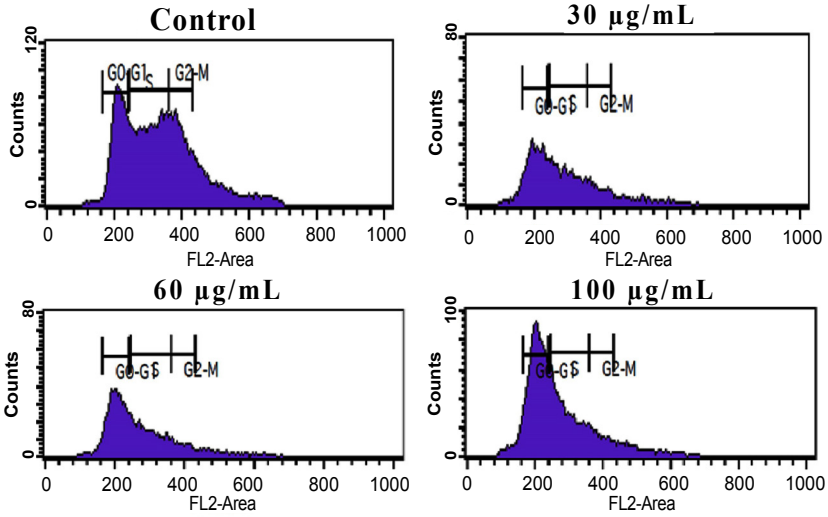

Figure 9: Cell cycle analysis of MCF-7 treated cells. Representative histograms demonstrate cell population according to the DNA content determined by propidium iodide staining. Control; 30 µg/ml; IC_{50} concentration (60 µg/ml) 24h; Maximum concentration (100 µg/ml).

cycle after treatment of MCF-7 cells G1 cell cycle arrest and increased cellular toxicity and apoptosis of the G0/G1 phase of cycle decreased and G2/M phase of cells increased [28].

Conclusion

In conclusion, we have demonstrated that green synthesis AgNPs from algal extract of Spirulina *platensis* inhibited the proliferation and induced apoptosis in MCF-7 breast cancer cell line. Due to weak chemical interaction with components of algal extract, the AgNPs are released *in vitro* leading to cytotoxic effects against human breast cancer cell. The algal extract capped nanoparticles solution was cytotoxic to MCF-7 cells in a concentration manner. The results suggest that AgNPs stimulates apoptosis through G0/G1cell cycle arrest. This was obviously due to DNA damage and elevated indices of oxidative stress in AgNPs treated cells. Therefore, biologically synthesized silver nanoparticles can be used for the treatment of cancer cells and can be exploited further to deliver drugs.

Acknowledgments

This work was financially supported by UGC-NON-SAP (G2/6966/UGC NON-SAP (Zoology)/2010) New Delhi, Govt. of India. The authors greatly acknowledged DRDO Centre for Life Sciences for nanoparticles characterization studies, Electron Microscopy Centre, AIIMS, New-Delhi. The authors are very much thankful to all faculty members of the Department of Zoology, Bharathiar University for their constant support and encouragement throughout this study.

References

1. Ahmad, Mukherjee P, Senapati S, Mandal D, Kumar MIKR, et al. (2003) Extracellular biosynthesis of silver nanoparticles using the fungus *Fusarium oxysporum.* Colloids Surf B Biointerfaces 28: 313–318.
2. Jeong SH, Yeo SY, Yi SC (2005) The effect of filler particle size on the antibacterial properties of compounded polymer/silver fibers. J Mater Sci 40: 5407-5411.
3. Husseiny MI, El-Aziz MA, Badr Y, Mahmoud MA (2007) Biosynthesis of gold nanoparticles using Pseudomonas aeruginosa. Spectrochim Acta A Mol Biomol Spectrosc 67: 1003-1006.
4. Bhainsa KC, D'Souza SF (2006) Extracellular biosynthesis of silver nanoparticles using the fungus Aspergillus fumigatus. Colloids Surf B Biointerfaces 47: 160-164.
5. Singaravelu G, Arockiamary JS, Kumar VG, Govindaraju K (2007) A novel extracellular synthesis of monodisperse gold nanoparticles using marine alga, Sargassum wightii Greville. Colloids Surf B Biointerfaces 57: 97-101.
6. Hu R, Yong KT, Roy I, Ding H, He S, et al. (2009) Metallic Nanostructures as Localized Plasmon Resonance Enhanced Scattering Probes for Multiplex Dark Field Targeted Imaging of Cancer Cells. J Phys Chem C Nanomater Interfaces 113: 2676-2684.
7. Dimitrijevic NM, Bartels D, Jonah CD, Takahashi K, Rajh T (2001) Radiolytically Induced Formation and Optical Absorption Spectra of Colloidal Silver Nanoparticles in Supercritical Ethane. J Phys Chem 105: 954-959.
8. Yin, Ma H, Wang S, Chen S (2003) Electrochemical Synthesis of Silver Nanoparticles under Protection of Poly(N-vinylpyrrolidone). J Phy Chem B 107: 8898-8904.
9. Callegari, Tonti D, Chergui M (2003) Photochemically Grown Silver Nanoparticles with Wavelength-Controlled Size and Shape. Nano Lett 3: 1565-1568.
10. Naik RR, Stringer SJ, Agarwal G, Jones SE, Stone MO (2002) Biomimetic synthesis and patterning of silver nanoparticles. Nat Mater 1: 169-172.
11. Gardea-Torresdey JL, Parsons JG, Gomez E, Peralta-Videa JR, Troiani H, et al. (2002) Formation and Growth of Au Nanoparticles inside Live Alfalfa Plants. Nano Lett 2: 397-401.
12. Ntalli NG, Cottiglia F, Bueno CA, Alché LE, Leonti M, et al. (2010) Cytotoxic tirucallane triterpenoids from Melia azedarach fruits. Molecules 15: 5866-5877.
13. Bhimba BV, Agnel Defora Franco DA, Mathew JM, Jose GM, Joel EL, et al. (2012) Anticancer and antimicrobial activity of mangrove derived fungi Hypocrea lixii VB1. Chin J Nat Med 10: 77-80.
14. Valentin Bhimba, Vinod V, Cindhu Beulah M (2011) Biopotential of secondary metabolites isolated from marine sponge Dendrilla nigra. Asian Pac J Trop Dis 1: 299-303.
15. Miura N, Shinohara Y (2009) Cytotoxic effect and apoptosis induction by silver nanoparticles in HeLa cells. Biochem Biophys Res Commun 390: 733-737.
16. Hsin YH, Chen CF, Huang S, Shih TS, Lai PS, et al. (2008) The apoptotic effect of nanosilver is mediated by a ROS- and JNK-dependent mechanism involving the mitochondrial pathway in NIH3T3 cells. Toxicol Lett 179: 130-139.
17. AshaRani PV, Low Kah Mun G, Hande MP, Valiyaveettil S (2009) Cytotoxicity and genotoxicity of silver nanoparticles in human cells. ACS Nano 3: 279-290.
18. Sukirtha R, Manasa Priyanka K, Antony JJ, Kamalakkannan S, Balasubramanian P (2012) Cytotoxic effect of Green synthesized silver nanoparticles using *Melia azedarach* against *in vitro* HeLa cell lines and lymphoma mice model .Process Biochemistry 47: 273-279.
19. Arjunan NK, Murugan K, Rejeeth C, Madhiyazhagan P, Barnard DR (2012) Green synthesis of silver nanoparticles for the control of mosquito vectors of malaria, filariasis, and dengue. Vector Borne Zoonotic Dis 12: 262-268.

20. Rejeeth, Nag TC, Kannan S (2013) Cisplatin-functionalized silica nanoparticles for cancer chemotherapy. Cancer Nano 4:127-136.

21. Tai KW, Chou MY, Hu CC, Yang JJ, Chang YC (2000) Induction of apoptosis in KB cells by pingyangmycin. Oral Oncol 36: 242-247.

22. Govindaraju K, Basha SK, Kumar VG, Singaravelu G (2008) Silver, gold and bimetallic nanoparticles production using single-cell protein (*Spirulina platensis*) Geitler. J Mater Sci 43: 5115-5122.

23. Vivek R, Thangam R, Muthuchelian K, Gunasekaran P, Kaveri K, et al. (2012) Green biosynthesis of silver nanoparticles from *Annona squamosa* leaf extract and its in vitro cytotoxic effect on MCF-7 cells. Process Biochemistry 47: 2405-2410.

24. Harekrishna B, Dipak KB, Gobinda V, Priyanka S, Misra PDA (2009) Green synthesis of silver nanoparticles using latex of *Jatropha curcas*. Colloids Surf A Physicochem Eng Asp 339: 134-139.

25. Das SK, Das AR, Guha AK (2009) Gold nanoparticles: microbial synthesis and application in water hygiene management. Langmuir 25: 8192-8199.

26. Nirmala R, Faheem AS, Kanjwal MA, Lee JH (2010) Synthesis and characterization of bovine femur bone hydroxyapatite containing silver nanoparticles for the biomedical applications. J Nanoparticle Res 10: 9944 - 9950.

27. Jain, Daima HK, Kachhwaha S, Kothari SL (2009) Synthesis of Plant-Mediated Silver Nanoparticles using Papaya Fruit Extract and Evaluation of their Anti Microbial Activities. J Nanomat Biostru 4: 723-727.

28. Roy P, Das S, Mondal A, Chatterji U, Mukherjee A (2012) Nanoparticle engineering enhances anticancer efficacy of andrographolide in MCF-7 cells and mice bearing EAC. Curr Pharm Biotechnol 13: 2669-2681.